10-1-2023

Energy, exergy, and economic evaluation of integrated waste incineration facility with a thermal power plant

Farid Aghapour sabagh

Siamak Hossainpour

Shayan Pourhemmati
Edith Cowan University

10.1016/j.ecmx.2023.100434
Hossainpour, S., & Pourhemmati, S. (2023). Energy, exergy, and economic evaluation of integrated waste incineration facility with a thermal power plant. Energy Conversion and Management: X, 20, 100434. https://doi.org/10.1016/j.ecmx.2023.100434

Energy Conversion and Management: X 20 (2023) 100434

Contents lists available at ScienceDirect

Energy Conversion and Management: X

journal homepage: www.sciencedirect.com/journal/energy-conversion-and-management-x

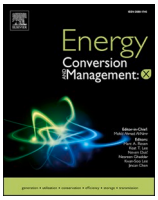

Energy, exergy, and economic evaluation of integrated waste incineration facility with a thermal power plant

Farid Aghapour sabagh [a], Siamak Hossainpour [a,*], Shayan Pourhemmati [b]

[a] Faculty of Mechanical Engineering, Sahand University of Technology, Tabriz, Iran
[b] School of Engineering, Edith Cowan University, 270 Joondalup Drive, WA 6027, Australia

ARTICLE INFO

Keywords:
Municipal solid waste incineration
Natural gas power plant
Waste to energy efficiency
Power plants integration

ABSTRACT

Increased waste production and poor waste management have created severe negative environmental impacts. Waste incineration is a way to produce energy and decreases environmental impacts; however, this technique cannot be considered independently as a source of power generation because of its low performance. This study aims to evaluate the integration of a waste incineration system with a natural gas-fired power plant in terms of energy, exergy, and economic points. As a result of the proposed configurations, in addition to promoting efficiency and net power production, some equipment is removed from power plants. Efforts are made to increase the accuracy of simulation results by paying attention to the combustion process in boilers and predicting the actual working condition of feed water heaters. Results showed that the hybrid scheme improves electricity generation by up to 2.87 MW and boosts energy, and exergy efficiency by up to 0.32%, and 0.3%, respectively.

1. Introduction

Disposing and eliminating MSW from residential, commercial, and institutional areas is a common problem in the modern world. This situation has been worsened by a growing population, economic development, changing consumption patterns, and rapid urbanization. The landfill is the cheapest way to manage a large amount of municipal waste. However, the lack of available land for disposal and environmental issues (emission of greenhouse gases such as methane) lead to public opposition to landfilling [1]. Prior experiences have proven that using only one management method to control waste problems cannot solve the general waste management problem. Therefore, the integrated waste management method is commonly used in developed countries [2]. In this method, elimination and utilizing solid waste for other purposes are possible at the same time. Fossil fuels generate more than 80% of electricity, and with increasing globalization and global warming, this method seems ineffective in providing sufficient electricity and decreasing the global warming effect [3,4]. MSW is considered an available renewable energy source to produce electricity. Two methods are used to turn MSW into energy; incineration and gasification. The first method utilizes a large amount of oxygen to provide energy and generates a considerable amount of energy, while the second procedure is economical and occurs in a low and limited amount of oxygen [5,6]. Incineration is a reliable way to produce thermal energy sources from solid waste [7]. This approach uses untreated waste as feedstock for energy production in waste incineration power plants. MSW incineration reduces the emission of greenhouse gases by preventing the landfill of large amounts of waste and can reduce fossil fuel consumption by producing a portion of energy demand in the power plants [8–10]. The thermal efficiency of WTE power plants is relatively low compared to conventional fossil fuel power plants, and even modern WTE power plants have low efficiency of around 22–25%. The reasons behind this are the small size of power plants, limited steam parameters (due to corrosion), high condensing pressure, simple configuration of power plants, stack loss due to the leaving of flue gases at high temperatures, and increased internal consumption of power plants [11]. Apart from that, advanced air pollution control systems are required to control the discharge of solid contents and acid gases from WTE boiler, which requires a high investment cost that developing countries cannot afford. The presence of salt and chlorine-containing plastics results in a total chlorine content of 0.2–2.5% in the MSW composition. These compounds are the main reason for high-temperature corrosion in MSW incineration [12,13]. Therefore, the live steam parameters of WTE plants are limited to 400–425 °C and 40–50 bar to mitigate this problem [14]. Apart from that, several techniques can be used to increase WTE efficiency and alleviate the poor performance of WTE plants, such as temperature reduction of flue gas leaving the boiler, employing an

* Corresponding author.
E-mail address: hossainpour@sut.ac.ir (S. Hossainpour).

https://doi.org/10.1016/j.ecmx.2023.100434
Received 20 May 2023; Received in revised form 12 July 2023; Accepted 4 August 2023
Available online 9 August 2023

Nomenclature

Symbols

$\dot{W}$	work rate (kW)
$\dot{E}x$	exergy rate (kW)
T	temperature (K)
$\dot{Q}$	heat transfer rate (kW)
M_w	molecular weight (kg/kmol)
$\dot{E}$	energy rate (kW)
R_g	universal gas constant (kJ/kmol K)
x_i	mole fraction (-)
h	specific enthalpy (kJ/kg)
$\dot{m}$	mass flow (kg/s)
s	specific entropy (kJ/kg)
C_p	specific thermal capacity (kJ/Kg K)

Abbreviations

FGR	flue gas recirculation
PAH	primary air heater
P	pump
EVA	evaporator
FG	flue gas
FWH	feed water heater
Cond	condenser
ECO	economizer
A	air
EF	exhaust fan
RHR	reheater
DEA	deaerator
BFP	boiler feed pump
LHV	lower heating value
IP	intermediate-pressure
HP	high-pressure
LMTD	logarithmic mean temperature difference
LP	low-pressure
GT	gas turbine
GEN	generator
MSW	municipal solid waste
NG	natural gas
NGPP	natural gas-fired power plant
APH	air pre-heater
AHPH	additional high-pressure heater
SA	secondary air
SAH	secondary air heater
SH	superheater
CP	condenser pump
APCS	air pollution control system
WIP	waste incineration pump
WIPP	waste incineration power plant
WTE	waste-to-energy
BF	blower fan
BA	bottom air

Subscript

b	boiler
ch	chemical
en	energy
ex	exergy
f	fuel
i	inlet
ic	internal consumption
ing	integrated
ke	kinetic
o	outlet
ph	physical
po	potential

Greek symbols

Ψ	mass exergy (kJ/kg)
η	efficiency (-)

external superheater, and exploiting refractory walls in the boiler to prevent corrosion.

Bogale et al. [14] investigated the impact of external superheaters on WTE power plants' performance. They increased live steam parameters to 540 °C and 135 bar and registered a maximum electrical efficiency of 33.19%. Considering conventional WTE plants with 86.5% boiler efficiency and 26.35% gross power efficiency, reducing the temperature of flue gases, leaving the boiler to 100 °C, promotes boiler efficiency and gross power efficiency to 92.63% and 28.14%, respectively [15]. Martin et al. [16] used corrosion-protected radiant superheaters to increase energy recovery. Since the electrical efficiency increases with rising live steam parameters, they achieved their goal and raised steam parameters to 50 bar and 440 °C. The impact of flue gas recirculation (FGR) on net power efficiency was investigated in the waste incinerator by Liuzzo et al. [17]. The FGR method resulted in a reduction of pollutant emissions by lowering the flue gas flow rate and led to the net power production efficiency being promoted by up to 15%. Several configurations of promoting WTE efficiency were evaluated by Eboh et al. [18]. In their work, the highest energy efficiency, up to 5%, was attained with the combination of waste gasification and flue gas condensation. Several studies have evaluated the possibility of improving WTE efficiency by integrating waste incineration boilers with various power generation systems.

Thermodynamic analysis of the integrated WTE boiler with the natural gas-fired boiler was investigated by Poma et al. [19], and the WTE efficiency was enhanced by up to 3%. In this configuration, the high-pressure stage of the turbine was extracted to preheat the air entering the waste incineration boiler, and a gas-fired boiler's superheater replaced the waste incineration boiler's superheater to produce superheated steam. Bianchi et al. [20] investigated the feasibility of increasing WTE efficiency by integrating the WTE power plant with a gas turbine. As a consequence of the proposed integration, the temperature and pressure of superheated steam increased to 514 °c and 80 bar, respectively, and positively affected the WTE efficiency. Chen et al. [21] combined the WTE system with the coal-fired power plant. The superheater of the WTE boiler was employed to heat the steam entering the IP turbine of the coal-fired power plant. Also, superheated steam leaving the WTE boiler was used to heat the feedwater entering the coal-fired boiler. As a result of the proposed configuration, WTE efficiency was promoted, and additional power was generated compared to conventional power plants. The feasibility of integrating the WTE system with the gas turbine cycle was evaluated by Carneiro et al. [22]. A heat recovery boiler integrated the gas-turbine cycle with the WTE system. The flue gas leaving the gas turbine was used for the combustion of natural gas in the second combustion chamber. Then combustion products were employed to heat the working fluid of the WTE boiler before entering the HP turbine. In the proposed hybrid WTE-GT system, WTE efficiency improved by up to 26%. Bianchi et al. [23] investigated the methods of repowering existing WTE power plants. Due to the inefficiency of the second boiler, the gas-turbine cycle was replaced by the second boiler. In the suggested configuration, the total power output increased from 25 MW to 54 MW, and WTE efficiency was promoted to 36%, which is more than conventional WTE plants.

Although previous investigations show positive outcomes in

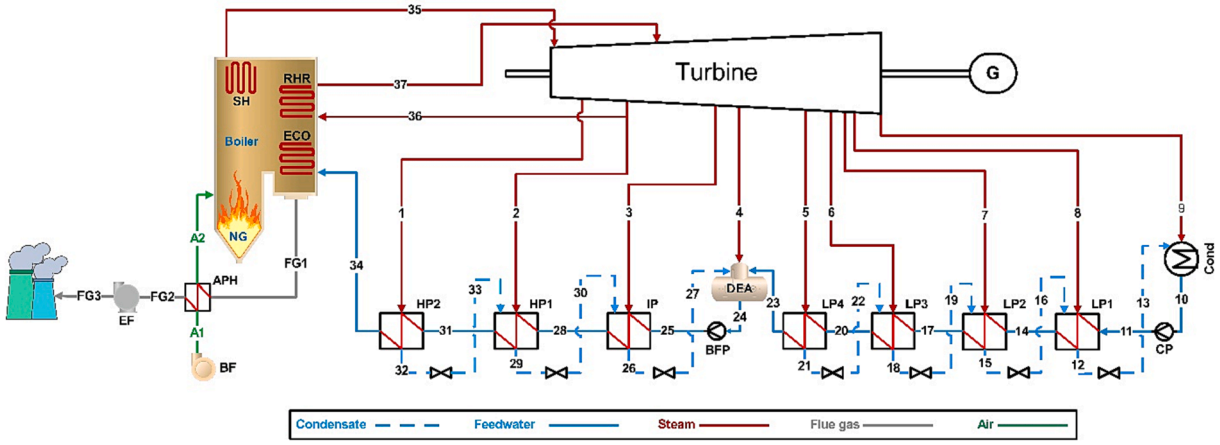

Fig. 1. Schematic of natural gas-fired power plant.

Table 1
Properties of natural gas.

Molecular weight	18.06 (gr/Mole)
LHV	45.3 (MJ/kg)
Components	
Methane	88.05 % (Mole)
Ethane	4.98 % (Mole)
Propane	1.14 % (Mole)
I-Butane	0.16 % (Mole)
n-Butane	0.22 % (Mole)
I-Pentane	0.07 % (Mole)
n-Pentane	0.05 % (Mole)
n-Hexane	0.03 % (Mole)
Carbon dioxide	0.73 % (Mole)
Nitrogen	4.57 % (Mole)

integrating power plants, the actual working conditions of feedwater heaters and the combustion process, to the best of our knowledge, are not considered. In the present work, efforts are made to increase the accuracy of simulation results by paying attention to these cases. Two hybrid combinations are proposed and evaluated regarding energy and exergy viewpoints. Also, an economic analysis of the proposed configuration is carried out to compare the equipment cost of the proposed models with conventional power plants. In order to fulfil this aim, the simulation of power plants is done by ASPEN HYSYS software, and the thermodynamics analysis of power plants is carried out in engineering equation solver software (EES).

2. Reference power plants

In this study, two working power plants are selected as references and new hybrid configurations are developed based on them. The data on natural gas-fired power plant (NGPP) is gathered from manufacturer. In contrast, due to the inaccessibility to waste incineration power plants (WIPP), the operational data is obtained from open literature [21].

2.1. Natural gas-fired power plan

A 350 MW natural gas-fired power plant (NGPP) is selected to integrate with a waste incineration power plant (WIPP). This power plant is located in the northwest of Iran and works stably in the design values. The schematic of the gas-fired power plant is shown in Fig. 1. In the boiler section, natural gas with a flow rate of 18.76 kg/s is combusted with 15% excess air to produce 308.7 kg/s of super-heated steam at

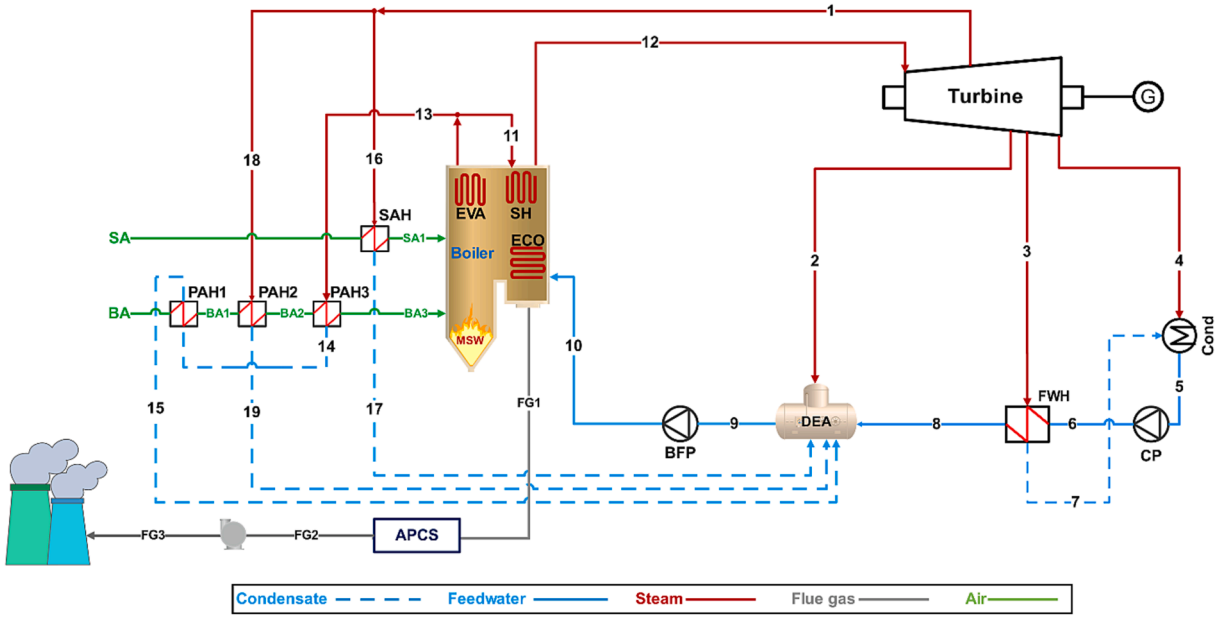

Fig. 2. Schematic of waste incineration power plant [21].

Table 2
Properties of MSW [21].

Molecular weight	20.04 (gr/Mole)
LHV	7 (MJ/kg)
Components	
Moisture	20.59 % (Mass)
Ash	41.75 % (Mass)
Carbon	21.97 % (Mass)
Hydrogen	1.91 % (Mass)
Oxygen	12.78 % (Mass)
Nitrogen	0.5 % (Mass)
Sulfur	0.2 % (Mass)
Chlorine	0.3 % (Mass)

Table 3
Comparison between reference and simulation results of selected WIPP.

Parameters	Present work	Ref. [21]	Difference (%)
MSW input rate (kg/s)	5.79	5.79	0
Turbine inlet steam			
Temperature (°C)	395	395	0
Pressure (bar)	39	39	0
Mass flow (kg/s)	13.5	13.5	0
Turbine outlet steam			
Temperature (°C)	38.49	38.5	− 0.01
Pressure (bar)	0.068	0.068	0
Mass flow (kg/s)	9.92	9.91	+ 0.01
Exhaust flue gas temperature (°C)	190	190	0
Boiler efficiency (%)	81.2	81	+ 0.2
Net power output (MW)	8.3	8.3	0
Thermal efficiency (%)	21.4	20.51	+ 0.91

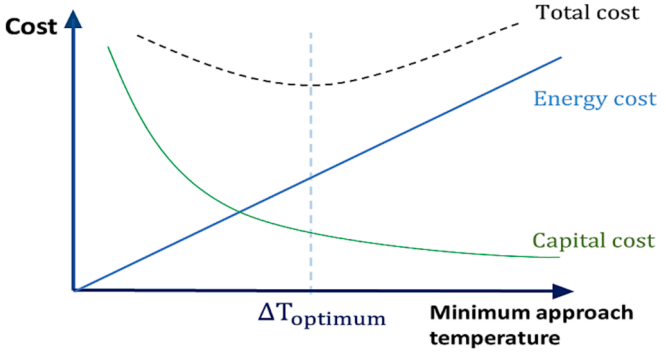

Fig. 3. The trade-off between energy cost and capital cost [24].

529 °C and 166 bar. The chemical composition of natural gas is listed in Table 1. The air (stream A2) is heated to 300 °C before entering the combustion chamber, and the combustion products pass through the boiler parts, namely the superheater, reheater, economizer, and air preheater, accordingly. The super-heated steam (stream 35) is introduced to the HP turbine, and then some part of it enters the RHR to receive additional heat before entering the IP turbine. The remaining steam flows to HP and IP feed water heaters. The expanded steam in the LP turbine condensates at the condenser and, after passing over the feed water heaters, pumps into the deaerator (DEA). Finally, the water leaving the DEA passes through the feed water heaters and pumps into the boiler. The detailed condition of steam in each point of the thermal power plant is presented in Table A.1 of Appendix A.

2.2. Waste incineration power plant

The operating waste incineration power plant (WIPP) in eastern China is selected to integrate with an NGPP. Fig. 2 illustrates the schematic of the power plant. The MSW with a 5.79 kg/s mass flow rate is used as fuel in the moving grate boiler. The chemical composition of MSW is listed in Table 2. The combustion products create 13.5 kg/s of superheated steam at 395 °C and 39 bar (stream 12) by passing through the evaporator, superheater, and economizer, respectively. The exhaust steam leaves the turbine, condensates at the condenser, and pumps into the boiler after passing the feedwater heaters. The evaporator is placed before the superheater in the boiler section to prevent high-temperature corrosion by keeping the flue gas temperature above 600 °C before entering the superheater. The detailed condition of steam in this cycle is presented in Table A.2 of Appendix A. The combustion air passes through the air pre-heaters before entering the boiler to better combustion. The primary and secondary air enters the boiler from the bottom and top of the grate, respectively. The energy needed for air preheaters is supplied by steam extracted from the evaporator and the steam extracted from the HP stage of the turbine [21].

3. Methodology

3.1. Validation and simulation method

This study aims to integrate WIPP with NGPP to promote waste-to-energy efficiency and the overall performance of a combined power plant. For this purpose, ASPEN HYSYS v11 is used to conduct a series of simulations. The numerical model accuracy is validated by comparing the obtained data with WIPP in Ref. [21], and the result is presented in Table 3. The simulation results of WIPP indicate a minor error in the thermal and boiler efficiencies. These discrepancies are due to the LHV of simulated MSW. The LHV of reference MSW is reported as 7 MJ/kg, while it is calculated as 6.7 MJ/kg in the ASPEN HYSYS simulation software. Since the boiler efficiency and net thermal efficiency are a function of LHV, the efficiencies will be changed by changing the LHV of the fuel. The heat exchanger simulation is done using a counter-current E-TYPE shell and tube heat exchanger, and its pressure loss in the shell side of heat exchangers is considered in the ranges from 3 to 5% [21]. The minimum temperature difference and the correction factor are assumed to be at least 5 °C and 0.75, respectively [24,25].

The minimum temperature difference in the heat exchanger is an important matter that can significantly impact the result. This is the minimum difference between cold and hot currents. In order to exchange heat between two fluids, there must be a minimum temperature difference between two fluids. Besides, the size of the heat exchanger is determined by the minimum temperature difference between the fluids; decreasing the temperature difference will result in a large size of the heat exchanger. Due to the energy cost and capital cost of heat exchangers, an optimum temperature difference is considered for heat exchangers. Since reducing the minimum temperature difference in the heat exchanger increases the heat transfer area and thus increases the investment cost of the heat exchanger, a practical temperature difference between 5 °C and 30 °C is considered for heat exchangers [24]. Table A.3 of Appendix A offers detailed information about heat exchangers. The trade-off scenario between energy cost and capital cost is shown in Fig. 3. The actual temperature difference is estimated in a heat exchanger by the LMTD correction factor (F_t). The correction factor is important in modelling shell and tube heat exchangers because it depends on the number of tubes, the temperature of the fluid in the shell and tubes, and the number of shells passes [24]. For a practical heat exchanger, the correction factor must be considered greater than 0.75 [25].

Simulations are carried out in two parts, the boiler and the steam cycle, and some assumptions for NGPP and WIPP are made, which are written as follows:

a) The Peng-Robinson and Soave-Redlich-Kong equation of state is used for NGPPs and WIPPs boilers, respectively and NBS stream table is used in the steam cycle.
b) The environmental states are considered 25 °C and 1.013 bar for temperature and pressure, respectively.

Table 4
Investment cost estimation of power plant's equipment.

Component	Function	Basic scale	Basic cost	Reference
Turbine	$C_T = 6000 \times (W_{ST})^{0.71}$	Power (kw)	K$	[21]
FWH	$C_{FWH} = 130 \times (A/0.093)^{0.78}$	Area (m^2)	K$	[34]
SH	$C_{SH} = 16500 \times (A/100)^{0.6}$	Area (m^2)	K$	[34]
ECO	$C_{Eco} = 3 \times 130 \times (A/0.093)^{0.78}$	Area (m^2)	K$	[34]
EVA	$C_{Eva} = 16000 \times (A/100)^{0.6}$	Area (m^2)	K$	[34]
Cond	$C_{Cond} = 8000 \times (A/100)^{0.6}$	Area (m^2)	K$	[34]
Gen	$C_{Gen} = 60 \times (P)^{0.95}$	Power (kw)	K$	[21]
DEA	$C_{DEA} = 6014 \times (m_f)^{0.7}$	Mass flow (kg/s)	K$	[21]
Pump	$C_P = 3540 \times (W_p)^{0.71}$	Power (kw)	K$	[21]
Stack	$C_s = 10645$	1122 (kg/s)	K$	[21]

Table 5
Conventional overall heat transfer coefficient [24].

Hot Fluid	Cold Fluid	U $(W/m^{2\circ}C)$
Heaters		
Water	Water	800 – 1500
Gases	Gases	10 – 50
Steam	Water	1500 – 4000
Steam	Gases	30 – 300
Flue gas	Steam	30 – 100
Condensers		
Aqueous Vapors	Water	1000 – 1500

c) The pressure loss on the heat exchangers' shell side is between 3 and 5%.
d) The heat losses of heat exchangers to the environment and the pressure loss in air preheaters are neglected.
e) Gibbs reactor is used to simulate the combustion chamber of NGPP, and the reaction equilibrium is calculated by minimizing the Gibbs free energy. The heat loss of the combustion chamber is neglected.
f) The turbine of NGPP and WIPP is simulated in several expansion stages, including two HP, two IP, and five LP stages. Each stage's inlet temperature and pressure are defined, and the extraction temperature and pressure determine the isentropic efficiency of each stage. The generator efficiency is assumed to be 99%.
g) The conversion reactor is used to simulate the combustion chamber of WIPP. Eqs. 1–3 defines the reactions in the combustion chamber [26]:

$$C + O_2 \rightarrow CO_2 \quad (1)$$

$$H_2 + 0.5\,O_2 \rightarrow H_2O \quad (2)$$

$$S + O_2 \rightarrow SO_2 \quad (3)$$

The operating temperature of the conventional waste incineration furnace is about 850 °C, which is good enough to form hydrogen chloride (HCl) [12]. The reaction of HCI formation in the MSW composition can be written as follow:

$$H_2 + Cl_2 \rightarrow 2HCl \quad (4)$$

h) The turbine of WIPP is simulated in several expansion stages, including an HP stage, an IP stage, and two LP stages. Each stage's inlet temperature and pressure are defined, and the extraction temperature and pressure determine the isentropic efficiency of each stage. The generator efficiency is assumed to be 99% [21].

3.2. Thermodynamic analysis

3.2.1. Energy

Thermodynamic analysis of a system investigates a system's balance of mass, energy, and exergy. Energy analysis of power generation systems is the ordinary method of performance assessment. By neglecting potential and kinetic energy in the steady-state process, the mass and energy balance of a system can be expressed by [27]:

$$\sum_i \dot{m}_i = \sum_o \dot{m}_o \quad (5)$$

$$\sum_i \dot{E}_i + \dot{Q} = \sum_o \dot{E}_o + \dot{W} \quad (6)$$

The boiler is an essential part of the power plant, and its efficiency affects the overall performance. Its efficiency is defined as the ratio of the practical heat output to the total energy input to the boiler and is expressed as [28]:

$$\eta_b = \frac{\dot{Q}_{out}}{\dot{Q}_{in}} \quad (7)$$

The energy efficiency (first law efficiency) of the power plant is defined as:

$$\eta_{en} = \frac{\dot{W}_{output}}{\dot{m}_f \times LHV} \quad (8)$$

The net power output of the system is written as follows:

$$W_{Net} = W_{out} - W_{ic} \quad (9)$$

where W_{out} is power produced by a power plant and W_{ic} is the total internal consumption of the power plant.

3.2.2. Exergy

Exergy is a maximum useful work that can be achieved when the system interacts with the environment, so that heat transfer occurs with the environment only. It measures the system's deviation from the environmental state and defines the quality of energy instead of quantity. Therefore, it is a property of the system and environment [29]. In general, exergy for a system is defined as follows:

$$ex = ex_{ph} + ex_{po} + ex_{ke} + ex_{ch} \quad (10)$$

The potential (ex_{po}) and kinetic (ex_{ke}) exergy are related to the height and motion of a system. For a steady-state system, they can be neglected [30]. The physical exergy is the maximum work that can be achieved by a system when it changes from the initial state to the dead state. The physical exergy can be defined as follows [29]:

$$ex_{ph} = (h - h_0) - T_0(s - s_0) \quad (11)$$

Where subscript 0 indicates the dead state.
The physical exergy of an ideal gas can be calculated as follows [31]:

$$ex = C_p\left[(T - T_0) - T_0 \ln\left(\frac{T}{T_0}\right)\right] + R_g T_0 \ln\left(\frac{P}{P_0}\right) \quad (12)$$

The chemical exergy is the maximum useful work that can be achieved when a system in a dead state reaches chemical equilibrium with the environment [29]. The chemical exergy of a gaseous mixture can be defined as follows [32]:

$$ex_{ch} = R_g T_0 \sum x_i \ln(x_i) + \sum x_i \dot{E}^{Ch}_{0,i} \quad (13)$$

The chemical exergy of a non-gaseous mixture can be expressed as follow:

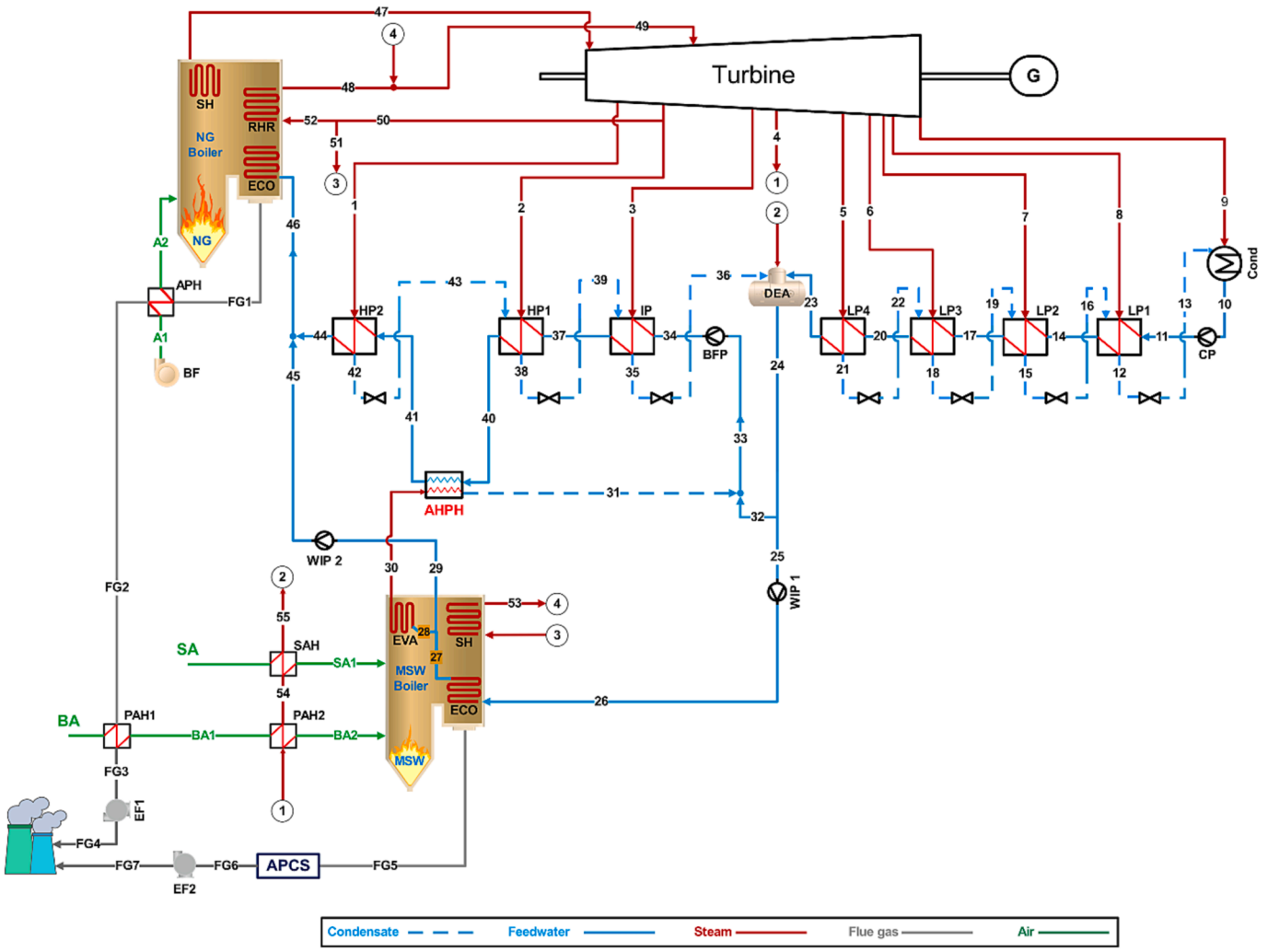

Fig. 4. The diagram of first configuration.

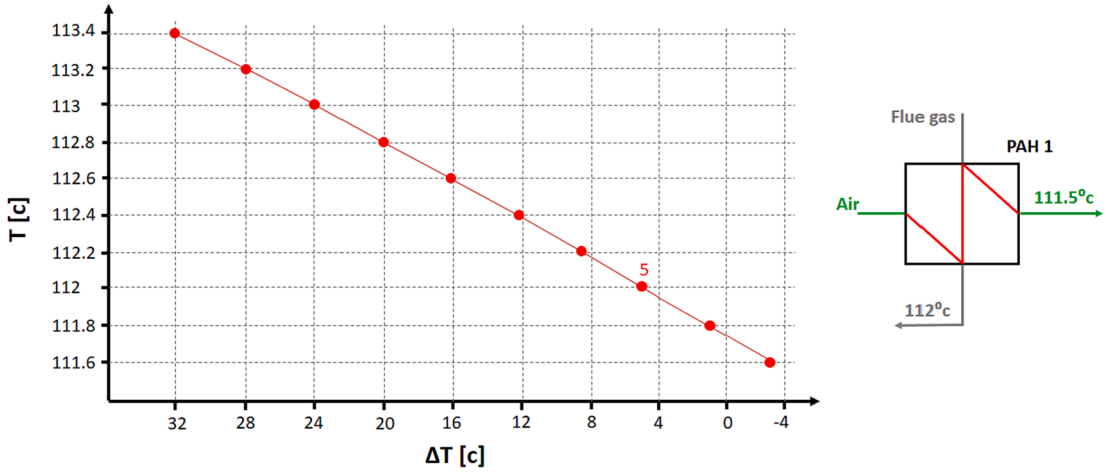

Fig. 5. Impact of flue gas outlet temperature on the minimum temperature difference of PAH1.

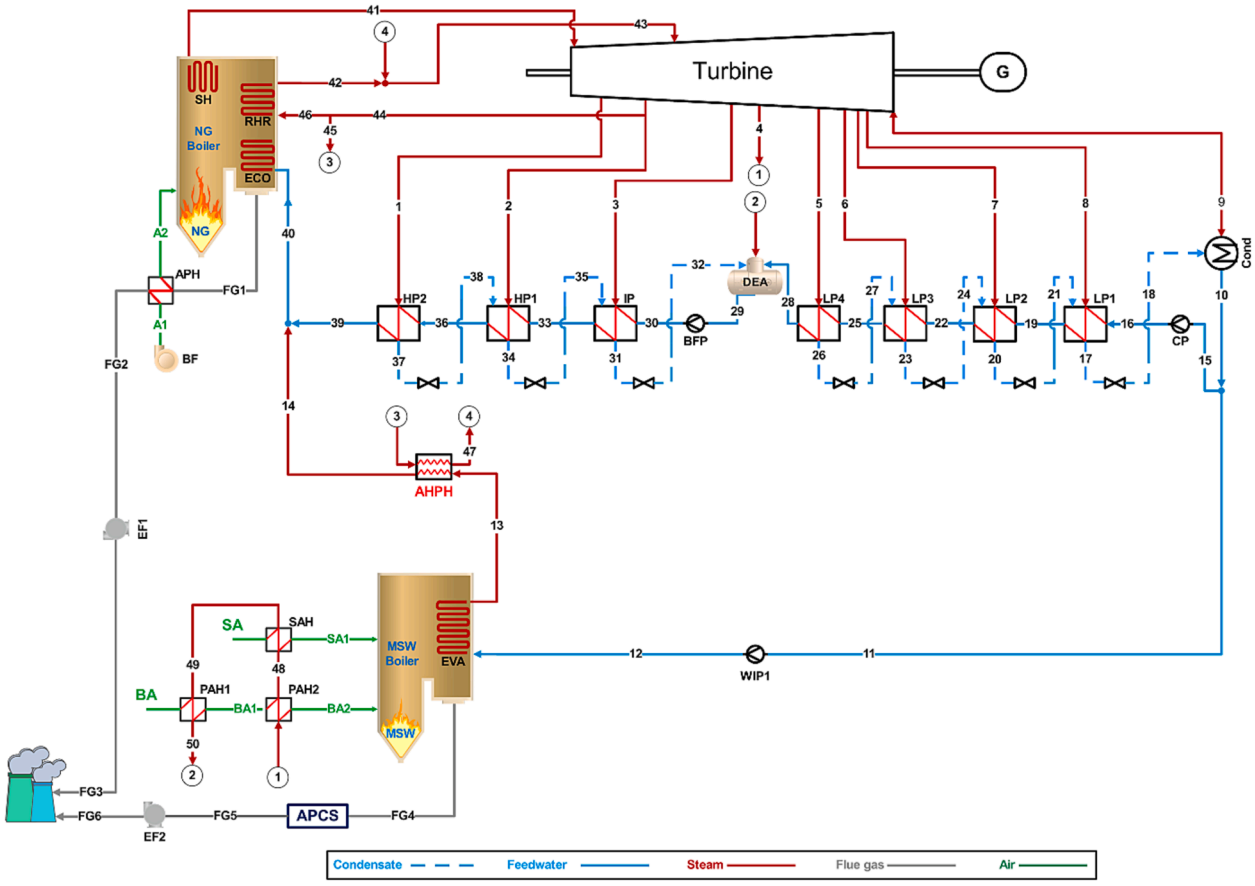

Fig. 6. The diagram of second configuration.

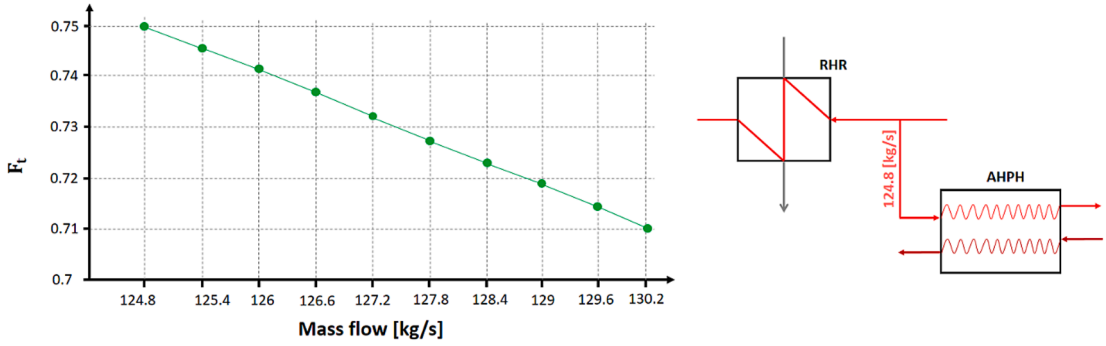

Fig. 7. The impact of extracted steam on the correction factor.

$$ex_{ch} = \sum x_i \dot{E}_{0,i}^{Ch} \tag{14}$$

Where $\dot{E}_{0,i}^{Ch}$ is the standard chemical exergy of a substance.

The exergy of natural gas and MSW is calculated by [21,33]:

$$ex_{NG} = \gamma_f \times LHV \tag{15}$$

$$\dot{E}x_{MSW} = \dot{m}_{MSW} \times \left(1.0064 + 0.1519 \times \frac{H}{C} + 0.0616 \times \frac{O}{C} + 0.0429 \times \frac{N}{C}\right) \times LHV_{MSW} \tag{16}$$

where $\gamma_f = 1.06$ and C, H, O and N are the mass percentage of carbon, hydrogen, oxygen and nitrogen, respectively.

3.3.3. Evaluation of integrated configuration

The energy efficiency of integrated systems is calculated by:

$$\eta_{en,ing} = \frac{\dot{W}_{ing}}{\dot{Q}_{MSW} + \dot{Q}_{NG}} \tag{17}$$

where $\dot{Q}_{MSW}$ and $\dot{Q}_{NG}$ are the energy of MSW and NG as a feedstock and equal to $\dot{m}_f \times$ LHV. The exergy efficiency of integrated systems is calculated as follows:

$$\eta_{ex,ing} = \frac{\dot{W}_{ing}}{\dot{E}x_{MSW} + \dot{E}x_{NG}} \tag{18}$$

The energy and exergy efficiency of waste-to-energy can be calculated by Eq. (19) and Eq. (20), respectively:

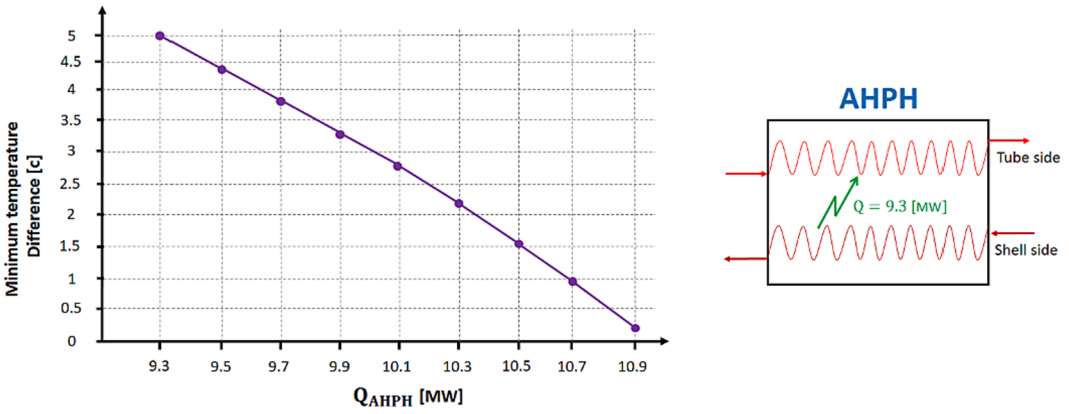

Fig. 8. The impact of heat transfer rate on the minimum temperature difference.

Table 6
First law analysis results.

	Separate-mode	First configuration	Second configuration
MSW flow rate (kg/s)	5.79	5.79	5.79
NG flow rate (kg/s)	18.76	18.76	18.76
MSW energy (Mw)	38.8	38.8	38.8
NG energy (Mw)	849.8	849.8	849.8
WTE boiler efficiency (%)	81.2	82	82
NG boiler efficiency (%)	93.7	93.7	93.7
Total gross power output (Mw)	353.7	355.5	356.1
Net power output of MSW (Mw)	8.3	8.6	11.2
Net power output of NG (Mw)	322.9	322.9	322.9
Total net power output (Mw)	331.2	331.5	334.1
WTE efficiency (%)	21.4	22.24	28.8
First law efficiency (%)	37.27	37.31	37.59

$$\eta_{WTE} = \frac{\dot{W}_{MSW}}{\dot{Q}_{MSW}} \tag{19}$$

$$\eta_{ex.WTE} = \frac{\dot{W}_{ing}}{\dot{E}x_{MSW}} \tag{20}$$

3.3. Economic analysis

As mentioned before, one of the aims of this study is to investigate possible economic advantages resulting from the integration. Therefore, the investment cost of a power plant's equipment must be specified. The equations for this purpose are presented in Table 4.

In order to estimate the investment cost of heat exchangers, the area of heat exchangers must be calculated. The following equation can be used for this purpose:

$$A = \frac{\dot{Q}}{U \times F_t \times \Delta T_{LMTD}} \tag{21}$$

$$\Delta T_{LMTD} = \frac{\left(T_{hot,in} - T_{cold,out}\right) - \left(T_{hot,out} - T_{cold,in}\right)}{\ln\left(\frac{T_{hot,in} - T_{cold,out}}{T_{hot,out} - T_{cold,in}}\right)} \tag{22}$$

The overall heat transfer coefficient is a function of a heat transfer process (conduction, convection, radiation), fluid properties inside the exchanger, and fluid flow rate. The conventional overall heat transfer coefficient in shell and tube heat exchangers is provided in Table 5.

4. Result and discussion

4.1. First configuration

The diagram of hybrid configuration is shown in Fig. 4. Some equipment of the waste incineration plant, such as the turbine, condenser, and feedwater heaters, are removed in the proposed configuration because of integration with the NGPP plant. As can be seen, the MSW and NG boilers have similar parts, namely, economizer, superheater, and air pre-heaters; however, in the MSW boiler evaporator is used, and in the NG boiler reheater is utilized. The MSW boiler is fed by a portion of the water leaving the deaerator. Thermal energy from the waste incineration boiler is transmitted to the steam cycle of the NG boiler using an additional high-pressure heat exchanger (AHPH). In this part, exhaust steam from the waste incineration boiler is condensed in the AHPH and returned to the steam cycle. As a consequence of this integration, the energy need of water entering the natural gas-fired boiler is met by both extraction steams and heat exchanged in the AHPH. So, the flow rate of extraction steam from the high-pressure stage of the turbine decreases, and the turbine's power output increases. Apart from that, A portion of the water entering the reheater in the NG boiler is extracted (point 3) from the steam cycle and employed in the waste incineration boiler. As a result, the temperature of the steam entering the IP turbine (point 4) is increased by receiving additional energy in the waste incineration superheater. The enhanced input steam temperature of the turbine results in an improvement in the turbine's power output. On the other hand, the wasted energy of the flue gas leaving the NG boiler is employed to heat the inlet air of the waste incineration boiler. As a result, the extraction steam of the IP turbine and the flue gas leaving the NG boiler meet the energy needs of the waste incineration air pre-heaters.

4.2. Parameter analysis of the first configuration

In the integrated system, corresponding to Fig. 4, the waste incineration economizer receives the water at 153.7 °C and 6.89 bar from the deaerator output and leaves it at 258 °C and 48.7 bar. A large part of the water is transmitted to the evaporator to finish the evaporation process, while the remaining water is returned to the steam cycle. Due to the limited parameters of the steam leaving the MSW superheater, a small quantity of water (29.14 kg/s) is extracted from the reheater section of the NG boiler inlet and transmitted to the superheater of the MSW boiler, leading the steam to exit the superheater at 395 °C. The detailed steam condition in this scheme and heat exchanger information are presented in Table A.4 and Table A.5 of Appendix A, respectively. The heat transferred in the AHPH enhanced the temperature of the water entering the NG boiler. The boiler efficiency is considered to be identical to that of conventional NGPP. In order to ensure that the water enters the NG

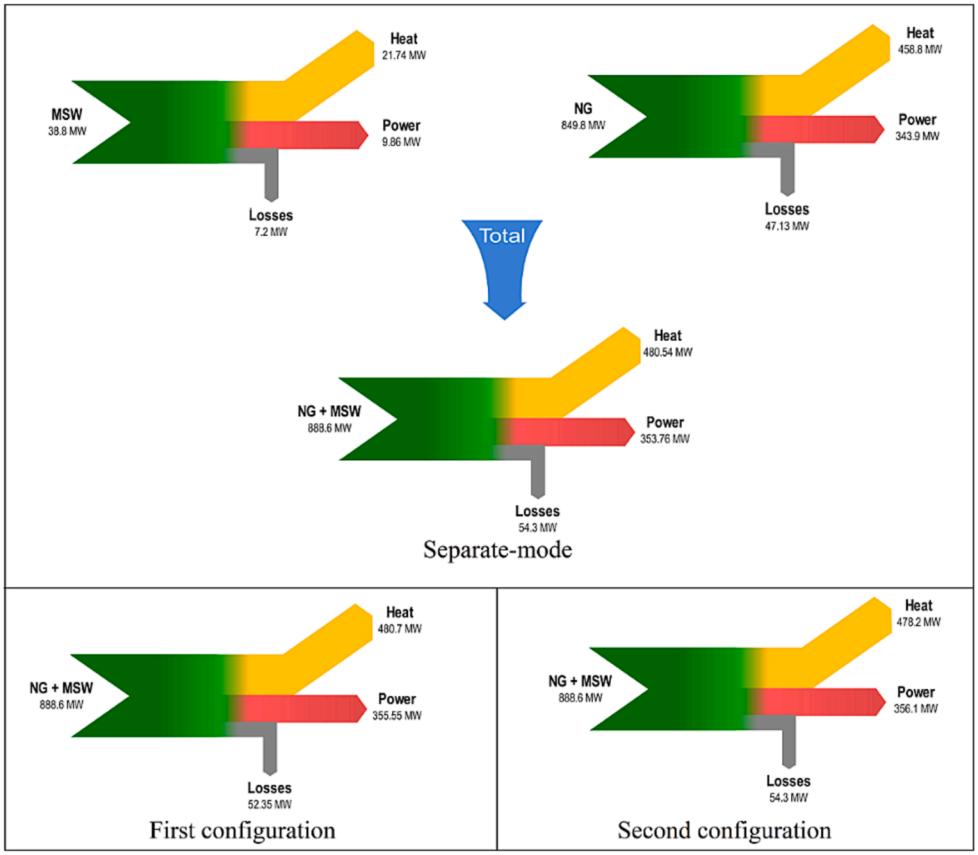

Fig. 9. Energy flow of power plants.

Table 7
Second law analysis.

	Separate-mode	First configuration	Second configuration
MSW exergy (MW)	40.9	40.9	40.9
NG exergy (MW)	900.8	900.8	900.8
Total exergy input (Mw)	941.7	941.7	941.7
Exergy output of MSW (MW)	8.3	8.6	11.2
Exergy output of NG (MW)	322.9	322.9	322.9
Total exergy output (MW)	331.2	331.5	334.06
WIPP exergy destruction (MW)	31.2	–	–
NGPP exergy destruction (MW)	563.4	–	–
Total exergy destruction (MW)	594.6	592.9	592.4
Second law efficiency (%)	35.17	35.2	35.47

boiler at the same conditions as the conventional NGPP, the mass flow of turbine extraction steam (stream 1) is reduced to 15.56 kg/s.

Since the air entering the MSW boiler could be heated by the flue gas leaving the NG boiler, one of the air preheaters in the WTE boiler is removed. The corrosion of boiler and stack metal surfaces is possible if the low temperature of flue gas leads to the condensation of acid gases. Therefore, due to the presence of water vapour in the flue gas, the maximum energy can be obtained above the dew point of the flue gas [35]. Otherwise, the minimum temperature difference of the PAH 1 is assumed to be at least 5 °C. So, the temperature of the flue gas leaving the air preheater is limited to 112 °C, and pre-heated air leaves the air pre-heater at 111.5 °C. The impact of flue gas outlet temperature on the minimum temperature difference is presented in Fig. 5, and detailed information is presented in Table A.6 of Appendix A. As can be seen, the flue gas temperature can be reduced to 111.8 °c, but in this case, the minimum temperature difference becomes below 5 °C, which leads to an increment in the area and investment cost of the heat exchanger. Also, by reducing temperature below 111.8 °c, the cold fluid outlet of the heat exchanger becomes hotter than the hot fluid inlet, and temperature-cross occurs, which is not practical for the heat exchangers [24,25].

4.3. Second configuration

Similar to the first configuration, the MSW boiler is integrated with an NGPP, and an AHPH is added to the system for thermal energy exchange between the two systems. The diagram of the second layout is demonstrated in Fig. 6, and the detailed condition of steam and heat exchangers in this cycle is presented in Table A.7 and Table A.8 of Appendix A, respectively. This layout removes the superheater and the economizer from the waste incineration boiler. Also, instead of extracting water from the deaerator, a portion of water leaving the condenser (stream 11) is used to import to the waste incineration boiler. After heating in the evaporator, water discharges from the waste incineration boiler in the vapour state (stream 13) and enters AHPH. In this section, heat transferring occurs and then the steam mix with high-pressure water and enters to economizer section of the NG boiler. The delivered heat in AHPH increases the steam temperature in the reheater section of the steam cycle. Similar to the previous configuration, a specified amount of steam is extracted from the turbine and, after the increasing temperature in AHPH, returns to the turbine's intermediate pressure stream, while the superheater is utilized to do this responsibility in the first configuration. As a result of the improved inlet temperature of the IP turbine, the power output of the turbine increases.

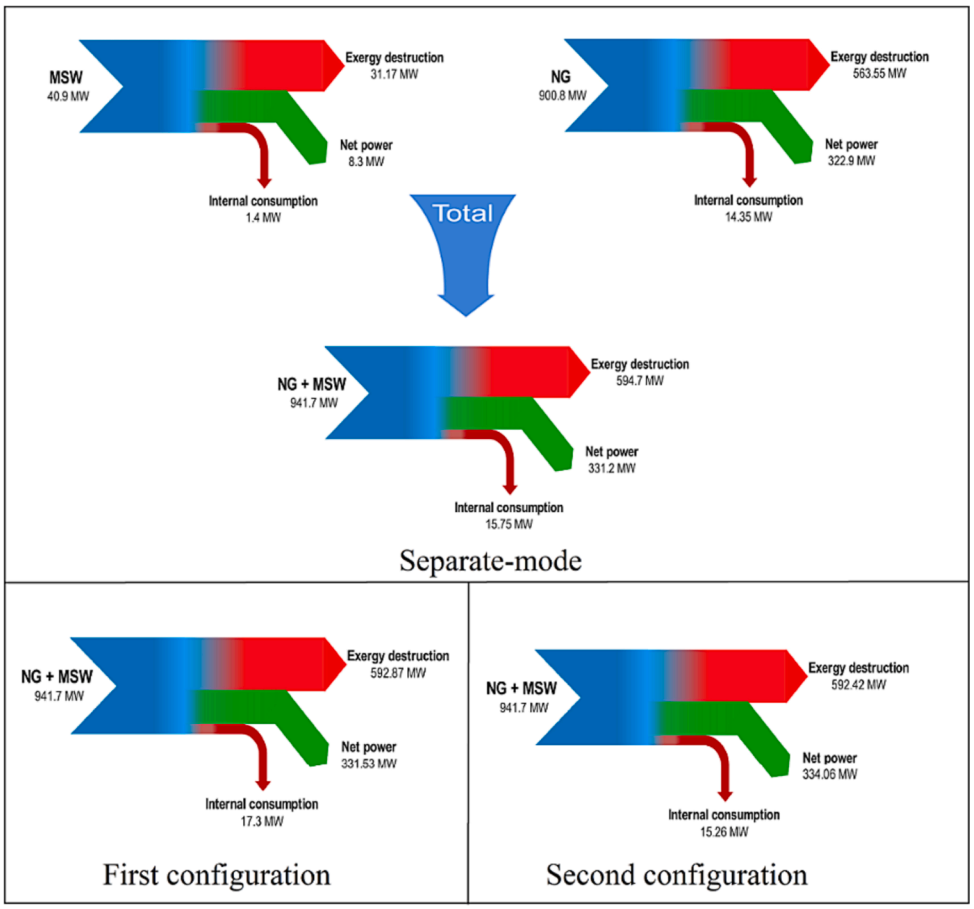

Fig. 10. Exergy flow of power plants.

Table 8
Internal consumption of power plants.

	Separate-mode	Configuration 1	Configuration 2
BFP1 (MW)	6.84	6.75	6.4
BFP2 (MW)	–	0.1	0.3
BFP3 (MW)	–	0.06	–
CP (MW)	0.5	0.5	0.47
EF1 (MW)	6.07	7.53	6.07
EF2 (MW)	0.6	0.6	0.25
BF (MW)	1.04	1.04	1.04
WTE internal consumption (MW)	0.7	0.7	0.7
Total consumption	15.75	17.3	15.26

BFP1: In the separate-mode indicates the power consumed by boiler feed water pump of NGPP and WIPP.
EF: EF1 is related to NG boiler and EF2 is related to WTE boiler.

4.4. Parameter analysis of the second configuration

In the second combined system, corresponding to Fig. 6, in order to promote the parameters of steam entering the IP section of the turbine, a portion of return steam (stream 44) is extracted from the steam cycle and navigated to the AHPH. The mass flow of extracted steam is limited to 124.8 kg/s in order to prevent the reduction of the RHR's correction factor below 0.75. The impact of extracted steam on the correction factor of RHR is displayed in Fig. 7, and detailed information is presented in Table A.9 of Appendix A. For a specific amount of extracted steam, the heat transfer rate in the AHPH is limited by the minimum temperature difference of the heat exchanger. As mentioned before, the minimum temperature difference of the heat exchanger is assumed to be at least 5 °C. So, the heat transfer rate in the AHPH is limited to 9.3 MW. The variation of heat transfer rate against the minimum temperature difference is demonstrated in Fig. 8. Further details are provided in Table A.10 of Appendix A.

4.5. Thermodynamic analysis

The proposed configurations are analyzed regarding thermodynamics' first and second laws. The results of the first law analysis are presented in Table 6, and the energy flow of power plants is shown in Fig. 9. In order to compare the performance of proposed configurations with conventional power plants, each plant's energy efficiency, exergy efficiency, and net power production are calculated separately. As shown in Table 6, both configurations have the same MSW and NG consumption rates. For a fair comparison, the boiler performance, including boiler efficiency and the air needed for combustion are kept the same as those in conventional power plants. The power produced by natural gas combustion is constant in both configurations, and the increment in the power generation is entirely due to the energy produced by waste incineration. Waste-to-energy efficiency is boosted in both new configurations, demonstrating the advantage of combining power plants. These increments for WTE are exactly 0.84% and 7.4% for the first and second configurations, respectively. Also, the overall efficiency of the first and second configurations is increased by 0.04% and 0.32%, respectively. According to the results of the first law, the second configuration performs better than the first configuration. So, the second configuration is chosen as the best-proposed configuration from the first law of thermodynamics perspective. The reason for increasing WTE boiler efficiency by 0.8 % in the new configuration is the different

Table 9
Investment cost of main equipment.

Equipment	Separate-Mode	First configuration	Second configuration
LP_1	82.9	79.9	87.2
LP_2	69.6	65.5	75.1
LP_3	62.4	57.6	69
LP_4	29.1	27.7	29.8
IP	144.9	112.8	131
HP_1	132	110	131.6
HP_2	48.8	37.2	34.7
AHPH	–	120.5	48.2
$Cond_{NGPP}$	216.8	227.4	225.5
Eco_{NGPP}	3012	3012	3012
SH_{NGPP}	186	186	186
RHR	138	140	184
APH	2918	2918	2918
DEA_{NGPP}	332.5	332.5	332.5
$Stack_{NGPP}$	3385	3688	3688
$Turbine_{NGPP}$	50,806	52,024	52,080
$Generator_{NGPP}$	10,702	11,046	11,062
CP_{NGPP}	288.6	297	281.5
Eva	40.7	40.7	68.4
PAH_1	4.3	60	21.8
PAH_2	36	28	26
SAH	16.8	19.4	17.5
BFP_{NGPP}	1852	1852	1789
BFP_{WIPP}	9.47	–	–
FWH	13.2	–	–
$Cond_{WIPP}$	37.8	–	–
DEA_{WIPP}	38.4	–	–
$Stack_{WIPP}$	329	–	–
$Turbine_{WIPP}$	4079	–	–
PAH_3	28.6	–	–
CP_{WIPP}	88.4	–	–
$Generator_{WIPP}$	366.3	–	–
Eco_{WIPP}	548.7	674	–
SH_{WIPP}	43.3	52	–
WIP_1	–	93	216.4
WIP_2	–	62	–
Total cost [K$]	80,086	77,363	76,715

environmental conditions for power plants. Since the simulated power plants work in different countries and weather conditions, the reference power plants have been simulated in different temperature conditions. The WIPP in Ref. [21] operates at 15 °C and 1.013 bar, while in the proposed configurations and NGPP, the working condition is 25 °C and 1.013 bar. Therefore, the temperature of the air entering the WTE boiler is increased by 10 °C, leading to an increase of boiler efficiency by 0.8%.

The energy flow of power plants is illustrated in Fig. 9 to conceive better performance of power plants in terms of the first law of thermodynamics. As can be seen, the flue gas loss decreased to 52.35 MW in the first configuration, and the gross power output increased to 355.55 MW. In the second configuration, the heat losses decreased in the condenser, and the gross power output increased to 356.1 MW. The condenser's heat loss is changed in the proposed configurations due to a little modification in the mass flow and the quality of the water entering the condenser. The exergy analysis is also done in the equation engineering solver software (EES). The environmental conditions of power plants are analyzed in this work at 25 °C and 1.013 bar. The exergy analysis results are presented in Table 7. As can be seen, the total exergy and exergy outputs of natural gas in the proposed configurations are the same as in the separate mode. In the first configuration, the total exergy output is increased by 0.3 MW while the exergy destruction is decreased by 1.7 MW. So, the second law efficiency is improved by 0.03%. For the second configuration, the increment of exergy and exergy destruction reduction is 2.9 MW and 2.2 MW, respectively. The obtained overall exergy efficiency is 0.3% for the second configuration. Thus, we can conclude that the second configuration performs better than the first configuration from the first and second law perspectives.

As shown in Fig. 10, the internal consumption of the power plant for the first hybrid model is increased by 1.55 MW. As mentioned, the air

Table A1
Operating parameters of natural gas-fired power plant.

Stream	ṁ(kg/s)	P (bar)	T (°C)	h (kJ/kg)	S (kJ/kg K)	Ψ (kJ/kg)
1	25.07	69	395.1	3147	6.43	1232
2	30	39.4	323.3	3025	6.47	1098
3	11.8	16.3	429.9	3319	7.32	1140
4	10.28	7.33	234.4	3109	7.36	918.4
5	10.22	3.63	244.8	2954	7.4	751.2
6	9.06	1.64	172.1	2816	7.48	590.7
7	8.159	0.64	87.65	2656	7.51	421.4
8	6.595	0.22	62.15	2613	7.87	269.5
9	197.5	0.063	37.07	2467	8	90.9
10	231.55	0.063	37.07	155.2	0.53	0.9
11	231.55	18	37.2	157.2	0.53	2.7
12	34.03	0.21	61.13	255.9	0.84	8.4
13	34.03	0.071	39.51	255.9	0.85	5.5
14	231.55	15.75	56.31	237	0.78	7.9
15	27.44	0.61	86.37	361.7	1.15	23.3
16	27.44	0.23	63.7	361.7	1.16	20.5
17	231.55	13.5	77.88	327.1	1.05	18.8
18	19.28	1.56	112.6	472.2	1.44	45.4
19	19.28	0.65	88.4	472.2	1.45	42.6
20	231.55	11.25	100.9	423.6	1.31	35.7
21	10.22	3.45	138.4	582.2	1.72	73.3
22	10.22	1.67	114.8	582.2	1.73	70.9
23	231.55	9	125.7	528.3	1.6	59.5
24	308.7	7.33	161.1	680.7	1.95	102.6
25	308.7	175.9	163.9	702.5	1.96	122.1
26	66.87	14.3	196.1	834.6	2.3	155.4
27	66.87	8.12	171.1	834.6	2.3	153
28	308.7	174.2	195.7	840.3	2.26	169.1
29	55.07	38.3	247.8	1075	2.77	252.6
30	55.07	15.77	200.7	1075	2.8	244.5
31	308.7	172.5	240.9	1043	2.7	248.9
32	25.07	65.5	281.4	1243	3.08	329.7
33	25.07	41.23	252.2	1243	3.1	325.7
34	308.7	170.8	273.3	1198	2.97	316.4
35	308.7	166	529.1	3372	6.38	1474
36	253.63	39.4	323.3	3025	6.47	1098
37	253.63	30	528.1	3520	7.31	1344
A1	338	1.04	28	307.5	5.32	2.63
A2	338	1.013	300	613.2	6	86.3
FG1	356.8	0.92	348.2	745.6	6.7	116.9
FG2	356.8	0.89	116.5	441.8	6.1	2.35
FG3	356.8	1.013	131.5	460.9	6.16	17.57

entering the WTE boiler is heated by the flue gas leaving the NG boiler. Since the flue gas passing the PAH1 experiences a pressure drop along the heat exchanger, the power consumption of the exhaust fan in the NGPP increases, which leads to additional power consumption compared to the separate mode. The detailed statistics are presented in Table 8. In the second configuration, the power consumed by the boiler feed pumps and exhaust fans is decreased by about 0.5 MW, which reduces internal consumption. The internal consumption in the WIPP includes the air pollution control systems and other internal consumers but excludes the power consumed by pumps and fans. As indicated in Ref. [11], the internal consumption of WIPPs is commonly about 10–15% and can be increased depending on the treatments employed in the WIPPs.

4.4. Economic analysis

The equipment cost of NGPP and WIPP is equal to 74,406 and 5680 thousand dollars, respectively. In this case, the total cost is estimated at 80,086 thousand dollars. In the proposed configurations, some of the equipment is removed, and new ones replace some. In the first configuration, the condenser pump, boiler feed water pump, generator, turbine, stack, feed water heaters, condenser, and one of the air preheaters of WIPP is removed. Instead, the AHPH and new pumps are added to the system. Also, some heaters are replaced with new heaters with a different heat transfer area due to the change in the heat transfer ratio of the feed water heaters in the NGPP. In this case, the equipment cost is

Table A2
Operating parameters of waste incineration power plant.

Stream	ṁ(kg/s)	P (bar)	T (°C)	h (kJ/kg)	S (kJ/kg K)	Ψ (kJ/kg)
1	1.57	13.1	287.3	3014	6.94	951.5
2	0.97	2.75	195.4	2857	7.33	675.4
3	1.04	0.8	93.55	2665	7.43	453.7
4	9.92	0.068	38.49	2345	7.52	95.15
5	10.96	0.068	38.49	161.1	0.55	1.14
6	10.96	2.97	38.51	161.5	0.55	1.44
7	1.04	0.75	91.98	385.3	1.21	27.47
8	10.96	2.85	90.18	377.9	1.19	26.31
9	14.12	2.75	129.9	546	1.63	63.44
10	14.12	52	130.6	552.3	1.63	69.05
11	13.5	45.4	258.1	2797	6.02	1009
12	13.5	39	395	3203	6.77	1192
13	0.62	45.4	258.1	2797	6.02	1009
14	0.62	45.4	225.3	968.5	2.56	209.2
15	0.62	45.4	104.3	440.3	1.35	42.1
16	0.49	13.1	287.3	3014	6.94	951.5
17	0.49	13.1	82.59	346.8	1.1	21.87
18	1.08	13.1	287.3	3014	6.94	951.5
19	1.08	13.1	76.95	323.2	1.04	18.2
SA	8.38	1.013	15	293.3	5.28	0.17
SA1	8.38	1.013	166	461.1	5.72	26.8
BA	20.51	1.013	15	293.3	5.28	0.17
BA1	20.51	1.013	30.6	310.2	5.34	0.05
BA2	20.51	1.013	167.6	462.8	5.72	27.4
BA3	20.51	1.013	220	523.2	5.84	47.7
FG1	34.68	0.92	190	511	6.04	29.12
FG2	31.9	0.9	190	518.3	6.19	28.4
FG3	31.9	1.013	206.7	539.3	6.2	44.73

Table A3
Heat exchangers properties.

	F_t	ΔT_{min}(°C)	ΔP_{Shell}(bar)	ΔP_{Tube}(bar)
First Configuration				
LP 1	0.98	6.5	0.01	2.25
LP 2	0.98	11.3	0.03	2.25
LP 3	0.99	15.6	0.08	2.25
LP 4	0.91	39.9	0.18	2.25
IP	0.92	8.7	1.47	1.7
HP 1	0.98	12.8	0.1	1.7
HP 2	0.88	28	3.5	1.7
AHPH	0.93	5	1.36	1.7
Eco_{NG}	0.8	74.9	0.03	2.57
RHR	0.92	361.9	0.03	9.4
SH_{NG}	0.96	600.9	0.03	2.23
Eco_{MSW}	0.81	35.6	0.03	3.3
Eva_{MSW}	1	273.1	0.03	3.3
SH_{MSW}	0.81	72.7	0.03	6.4
APH	0.82	48.1	0.03	0.03
PAH 1	0.86	5	0.03	0
PAH 2	0.79	105.4	0.2	0
SAH	0.8	52.1	0.2	0
Second Configuration				
LP 1	0.97	5.1	0.01	2.25
LP 2	0.98	8.1	0.03	2.25
LP 3	0.98	10.6	0.08	2.25
LP 4	0.88	34.9	0.18	2.25
IP	0.87	6	1.47	1.7
HP 1	0.97	8.2	1.1	1.7
HP 2	0.91	40.1	3.5	1.7
AHPH	0.89	5	5.2	1.7
Eco_{NG}	0.8	74.9	0.03	2.57
RHR	0.75	238.7	0.03	9.4
SH_{NG}	0.96	600.9	0.03	2.23
Eco_{MSW}	–	–	–	–
Eva_{MSW}	0.9	151.6	0.03	3.3
SH_{MSW}	–	–	–	–
APH	0.82	48.1	0.03	0.03
PAH 1	0.98	59.5	0.2	0
PAH 2	0.82	111.8	0.2	0
SAH	0.83	58.3	0.2	0

Table A4
Operating parameters of first configuration.

Stream	ṁ(kg/s)	P (bar)	T (°C)	h (kJ/kg)	S (kJ/kg K)	Ψ (kJ/kg)
1	15.56	69	395.1	3147	6.44	1232
2	30	39.4	323.3	3025	6.48	1098
3	11.8	16.3	431.1	3321	7.33	1141
4	10.28	7.33	325.4	3111	7.37	919.6
5	10.22	3.63	245.7	2956	7.41	752.1
6	9.06	1.64	172.9	2817	7.48	591.3
7	8.16	0.64	88.35	2657	7.51	421.7
8	6.595	0.22	62.86	2614	7.88	269.7
9	207.03	0.06	37.07	2468	7.99	90.92
10	241.06	0.06	37.07	155.3	0.53	0.9
11	241.06	18	37.2	157.4	0.53	2.72
12	34.03	0.21	61.13	255.9	0.84	8.4
13	34.03	0.07	39.51	255.9	0.85	5.5
14	241.06	15.75	55.57	233.9	0.77	7.6
15	27.44	0.61	86.37	361.7	1.15	23.26
16	27.44	0.23	63.7	361.7	1.16	20.52
17	241.06	13.5	76.3	320.5	1.03	17.83
18	19.28	1.56	112.6	472.2	1.44	45.39
19	19.28	0.66	88.4	472.2	1.45	42.62
20	241.06	11.25	98.45	413.3	1.28	33.68
21	10.22	3.45	138.4	582.3	1.72	73.28
22	10.22	1.68	114.8	582.3	1.73	70.87
23	241.06	9	122.3	513.9	1.55	55.87
24	308.7	6.89	153.7	648.5	1.88	92.65
25	17.2	6.89	153.7	648.5	1.88	92.65
26	17.2	52	154.4	654.3	1.88	97.85
27	17.2	48.7	258	1125	2.86	274.9
28	14.11	48.7	258	1125	2.86	274.9
29	3.09	48.7	258	1125	2.86	247.9
30	14.11	45.4	258.1	2797	6	1009
31	14.11	44.04	256.2	1115	2.85	270.6
32	291.5	6.89	153.7	648.5	1.88	92.65
33	305.6	6.89	158.7	670.1	1.93	99.24
34	305.6	177.6	161.5	692.2	1.94	119
35	57.36	14.3	196.1	834.8	2.29	155.4
36	57.36	8.12	171.1	834.8	2.3	153
37	305.6	175.9	191.9	823.9	2.23	163.3
38	45.56	38.3	247.8	1075	2.77	252.6
39	45.56	15.77	200.7	1075	2.8	244.5
40	305.6	174.2	236.7	1024	2.64	240.8
41	305.6	172.5	253.3	1102	2.79	273.7
42	15.56	65.5	281.4	1243	3.08	329.7
43	15.56	41.23	252.2	1243	3.1	325.7
44	305.6	170.8	273.4	1199	2.97	316.6
45	3.09	170.8	262	1143	2.87	291.6
46	308.7	170.8	273.3	1198	2.97	316.4
47	308.7	166	529.1	3373	6.38	1474
48	234	30	546.5	3561	7.36	1370
49	263.14	30	529.4	3523	7.31	1345
50	263.14	39.4	323.3	3025	6.48	1098
51	29.14	39.4	323.3	3025	6.48	1098
52	234	39.4	323.3	3025	6.48	1098
53	29.14	33	395	3214	6.85	1175
54	10.28	7.11	217.7	2884	6.96	813
55	10.28	6.89	165.3	2765	6.71	766.4
A1	338	1.04	28	307.5	5.32	2.63
A2	338	1.013	300	613.2	6	86.3
SA	8.38	1.013	25	304.1	5.32	0
SA1	8.38	1.013	166	461.1	5.72	26.8
BA	20.51	1.013	25	304.1	5.32	0
BA1	20.51	1.013	111.5	399.2	5.58	10.9
BA2	20.51	1.013	220	523.2	5.84	47.69
FG1	356.8	0.92	348.2	745.6	6.69	116.9
FG2	356.8	0.89	116.5	441.8	6.16	2.35
FG3	356.8	0.86	112	435.2	6.15	−1.5
FG4	356.8	1.013	130.6	459.8	6.16	17.3
FG5	34.68	0.92	190	511.3	6.04	29.12
FG6	31.89	0.9	190	514.1	6.19	28.23
FG7	31.89	1.013	205.7	566.1	6.19	44.35

Table A5
Detailed heat exchanger information for Configuration 1.

	U (W/m^2.K)	Basic scale	Unit	K$
LP1	4000	350	A (m^2)	79.9
LP2	4000	271	A (m^2)	65.5
LP3	4000	230	A (m^2)	57.6
LP4	4000	90	A (m^2)	27.7
IP1	4000	544	A (m^2)	112.8
HP1	4000	530	A (m^2)	110
HP2	4000	131	A (m^2)	37.2
AHPH	4000	592	A (m^2)	120.5
Condenser	1500	26,481	A (m^2)	227.4
Eco NG	100	8972	A (m^2)	3012
SH NG	100	5666	A (m^2)	186
RH	100	3528	A (m^2)	140
APH NG	50	35,222	A (m^2)	2918
Eco WTE	100	1316	A (m^2)	674
SH WTE	100	672	A (m^2)	51.7
Eva	100	475	A (m^2)	40.7
APH1	300	244	A (m^2)	60
APH2	300	92	A (m^2)	28
SPH	300	57	A (m^2)	19.4
				Others
		Basic scale	Unit	K$
	DEA	308.7	Kg/s	332.5
	Stack	388.7	Kg/s	3688
	Turbine	352,000	Kw	52,023
	Generator	348,480	Kw	11,046
	Pump DEA	6753	Kw	1853
	Pump Cond	512	Kw	297
	Pump WTE 1	100	Kw	93
	Pump WTE 2	56	Kw	62
			Total	77,363

Table A6
Impact of flue gas outlet temperature on the minimum temperature difference of PAH1.

Point	$T_{flue\ gas}$(°C)	ΔT (°C)
1	111.6	−3.1
2	111.8	0.27
3	112	5.02
4	112.1	7.23
5	112.3	10.72
6	112.5	14.21
7	112.7	17.70
8	112.9	21.18
9	113	24.67
10	113.2	28.16
11	113.4	31.65
12	113.6	35.15
13	113.7	38.64
14	113.9	42.14
15	114.1	45.63
16	114.3	49.13
17	114.5	52.63
18	114.6	56.13
19	114.8	59.62
20	115	63.12

reduced to 77,363 thousand dollars. In the second layout, the WTE boiler's superheater and economizer are removed in addition to the other equipment mentioned in the first configuration, keeping only the evaporator in use as a steam generator. In this case, the equipment cost is reduced to 76,715 thousand dollars. As a result of the proposed configurations, the main equipment cost of the power plant is lessened by 2723 and 3371 thousand dollars for the first and the second configuration, respectively. Detailed information is provided in Table 9.

Table A7
Operating parameters of second configuration.

ddStream	ṁ(kg/s)	P (bar)	T (°C)	h (kJ/kg)	S (kJ/kg K)	Ψ (kJ/kg)
1	17.3	69	395	3147	6.43	1232
2	30	39.4	323.3	3025	6.47	1098
3	11.8	16.3	438.3	3337	7.35	1151
4	10.28	7.33	331.8	3125	7.38	926.3
5	10.22	3.63	251.4	2968	7.43	757
6	9.06	1.64	177.9	2828	7.5	594.6
7	8.159	0.64	92.44	2666	7.53	423.1
8	6.595	0.22	66.99	2622	7.9	270.6
9	205.15	0.06	37.07	2475	8.01	91.2
10	239.18	0.06	37.07	155.3	0.53	0.9
11	15.75	0.06	37.07	155.3	0.53	0.9
12	15.75	179.3	38.35	176.5	0.54	19.01
13	15.75	176	355.9	2539	5.15	1006
14	15.75	170.8	352.7	1957	4.21	694.4
15	223.57	0.06	37.07	155.3	0.53	0.9
16	223.57	18	37.2	157.4	0.53	2.7
17	34.03	0.21	61.13	255.9	0.84	8.4
18	34.03	0.07	39.5	255.9	0.85	5.5
19	223.57	15.75	57.06	240.3	0.79	8.2
20	27.44	0.61	86.37	361.7	1.15	23.2
21	27.44	0.23	63.7	361.7	1.16	20.5
22	223.57	13.5	79.47	334	1.06	19.8
23	19.28	1.56	112.6	472.2	1.44	45.39
24	19.28	0.65	88.4	472.2	1.45	42.6
25	223.57	11.25	103.4	434.5	1.34	37.9
26	10.22	3.45	138.4	582.3	1.72	73.3
27	10.22	1.68	114.8	582.3	1.73	70.8
28	223.57	9	129.2	543.4	1.62	63.28
29	292.95	6.68	159.7	674.8	1.94	100.5
30	292.95	175.9	162.4	696.9	1.94	120.2
31	59.1	14.3	196.1	834.7	2.29	155.4
32	59.1	8.12	171.1	834.7	2.3	153
33	292.95	174.2	194.7	836.4	2.25	167.4
34	47.3	38.3	247.8	1075	2.77	252.6
35	47.3	15.77	200.7	1075	2.8	244.5
36	292.95	172.5	241.3	1045	2.68	249.7
37	17.3	65.5	281.4	1243	3.08	329.7
38	17.3	41.23	252.2	1243	3.09	325.7
39	292.95	170.8	265.1	1158	2.89	298.3
40	308.7	170.8	273.3	1198	2.97	316.4
41	308.7	166	529.1	3373	6.38	1474
42	136.63	30	713.7	3939	7.79	1626
43	261.4	30	537.4	3541	7.34	1357
44	261.4	39.4	323.2	3025	6.47	1098
45	124.8	39.4	323.2	3025	6.47	1098
46	136.6	39.4	323.2	3025	6.47	1098
47	124.8	37.7	350.9	3099	6.61	1131
48	10.28	7.11	224.3	2897	6.98	818.3
49	10.28	6.89	170.9	2778	6.74	770.7
50	10.28	6.68	163.1	2601	6.35	710.4
A1	338	1.04	28	307.5	5.32	2.63
A2	338	1.013	300	613.2	6	86.3
SA	8.38	1.013	25	304.1	5.32	0
SA1	8.38	1.013	166	461.1	5.72	26.8
BA	20.51	1.013	25	304.1	5.32	0
BA1	20.51	1.013	111.5	399.2	5.58	10.9
BA2	20.51	1.013	220	523.2	5.84	47.69
FG1	356.8	0.92	348.2	745.6	6.69	116.9
FG2	356.8	0.89	116.5	441.8	6.16	2.35
FG3	356.8	1.013	131.5	460.9	6.16	17.57
FG4	34.68	0.98	190	513.6	6.02	34.3
FG5	31.89	0.96	190	518.2	6.17	32.9
FG6	31.89	1.013	196.6	526.1	6.17	40.4

5. Conclusion

The 350 MW natural gas-fired power plant is integrated with a 9.86 MW waste incineration power plant in two different configurations. The proposed layouts are analyzed using ASPEN HYSYS and EES software from economic and thermodynamics laws viewpoints. Two parameters are hired for heat exchangers to predict the actual working condition; the first one is the temperature difference range for two fluids, which is

Table A8
Detailed heat exchanger information for Configuration 2.

	U (W/m^2.K)	Basic scale	Unit	K$
LP1	4000	391	A (m^2)	87.2
LP2	4000	323	A (m^2)	75.1
LP3	4000	290	A (m^2)	69
LP4	4000	99	A (m^2)	29.8
IP1	4000	662	A (m^2)	131
HP1	4000	663	A (m^2)	131.6
HP2	4000	120	A (m^2)	34.7
AHPH	4000	183	A (m^2)	48.2
Condenser	1500	26,111	A (m^2)	225.5
Eco NG	100	8972	A (m^2)	3012
SH NG	100	5666	A (m^2)	186
RH	100	5583	A (m^2)	184
APH NG	50	35,222	A (m^2)	2918
Eva	100	1125	A (m^2)	68.4
APH1	300	66	A (m^2)	21.8
APH2	300	84	A (m^2)	26
SPH	300	50	A (m^2)	17.5
	Other	Basic scale	Unit	K$
	DEA	308.7	Kg/s	332.5
	Stack	388.7	Kg/s	3688
	Turbine	352,550	Kw	52,080
	Generator	349,024	Kw	11,062
	Pump DEA	6425	Kw	1789
	Pump Cond	475	Kw	281.5
	Pump WTE 1	328	Kw	216.4
			Total	76,715

Table A9
The impact of extracted steam on the correction factor.

Point	Mass flow [kg/s]	F_t
1	123.8	0.749
2	124.1	0.754
3	124.5	0.751
4	124.8	0.749
5	125.1	0.747
6	125.4	0.745
7	125.8	0.742
8	126.1	0.740
9	126.4	0.738
10	126.7	0.736
11	127.1	0.733
12	127.4	0.731
13	127.7	0.728
14	128	0.726
15	128.4	0.723
16	128.7	0.721
17	129	0.718
18	129.3	0.715
19	129.7	0.712
20	130.2	0.71

between 5℃ and 30℃. The second parameter is the correction factor, assumed to be at least 0.75 in the present work. The detailed analysis of the combustion in chambers is done by considering Gibbs reactor for NGPP and conversion reactor for WIPP. The results indicate that the second layout performs better than the first one. The detailed outcomes of this study are presented in the following:

- In the first configuration, the superheated steam leaving the waste incineration boiler is utilized to increase the temperature of water feeding into the natural gas-fired boiler. In this case, the power plant's power output, energy efficiency, and waste-to-energy efficiency are increased by 0.33 MW, 0.04%, and 0.84%, respectively. In addition, the total exergy destruction of power plants is diminished by 1.74 MW, and the exergy efficiency increased by 0.03%. Due to the removal of some equipment in the waste-to-energy plant, the total investment cost of the power plant is lessened by 2.68%.

Table A10
The impact of heat transfer rate on the minimum temperature difference.

Point	Q_AFWH[kw]	Minimum temperature difference [C]
1	9300	5.065
2	9418	4.681
3	9512	4.378
4	9605	4.074
5	9699	3.771
6	9792	3.467
7	9886	3.163
8	9979	2.859
9	10,072	2.555
10	10,166	2.251
11	10,259	1.946
12	10,353	1.642
13	10,446	1.337
14	10,539	1.032
15	10,633	0.7276
16	10,726	0.4226
17	10,820	0.2175
18	10,913	0.1002
19	11,007	−0.493
20	11,100	−0.7985

- In the second configuration, the superheated steam leaving the waste incineration boiler is utilized to increase the temperature of steam feeding into the IP turbine and the water feeding into the natural gas-fired boiler. In this case, the power output of the power plant, energy efficiency, and waste-to-energy efficiency is increased by 2.9 MW, 0.32%, and 7.4%, respectively. In addition, the total exergy destruction of power plants is alleviated by 2.2 MW and the exergy efficiency is boosted by 0.3%. Eliminating some equipment, such as the superheater and the economizer, from the waste incineration boiler decreases the investment cost by 4%.

CRediT authorship contribution statement

Farid Aghapour sabagh: Software, Data curation, Writing – original draft, Visualization, Investigation, Validation, Writing – review & editing, Formal analysis. **Siamak Hossainpour:** Supervision, Conceptualization, Methodology, Writing – review & editing, Visualization, Investigation, Resources. **Shayan Pourhemmati:** Software, Data curation, Writing – original draft, Writing – review & editing, Formal analysis.

Declaration of Competing Interest

The authors declare that they have no known competing financial interests or personal relationships that could have appeared to influence the work reported in this paper.

Data availability

No data was used for the research described in the article.

Appendix A

References

[1] Tan ST, Ho WS, Hashim H, Lee CT, Taib MR, Ho CS. Energy, economic and environmental (3E) analysis of waste-to-energy (WTE) strategies for municipal solid waste (MSW) management in Malaysia. Energ Conver Manage 2015;102:111–20.
[2] Zaman AU. Comparative study of municipal solid waste treatment technologies using life cycle assessment method. Int J Environ Sci Technol 2010;7:225–34. https://doi.org/10.1007/BF03326132.
[3] Makarichi L, Jutidamrongphan W, Techato K-A. The evolution of waste-to-energy incineration: A review. Renew Sustain Energy Rev 2018;91:812–21.

[4] Song Q, Wang Z, Li J, Duan H, Yu D, Liu G. Comparative life cycle GHG emissions from local electricity generation using heavy oil, natural gas, and MSW incineration in Macau. Renew Sustain Energy Rev, Elsevier 2018;81(P2):2450–9.
[5] Fernández-González JM, Grindlay AL, Serrano-Bernardo F, Rodríguez-Rojas MI, Zamorano M. Economic and environmental review of Waste-to-Energy systems for municipal solid waste management in medium and small municipalities. Waste Manag 2017;67:360–74.
[6] Arafat H, Jijakli K. Modeling and comparative assessment of municipal solid waste gasification for energy production. Waste Manag 2013;33(8):1704–13. https://doi.org/10.1016/j.wasman.2013.04.008.
[7] Dong J, Tang Y, Nzihou A, Chi Y, Weiss-Hortala E, Ni M. Life cycle assessment of pyrolysis, gasification and incineration waste-to-energy technologies: Theoretical analysis and case study of commercial plants. Sci Total Environ 2018;626:744–53. https://doi.org/10.1016/j.scitotenv.2018.01.151.
[8] Rand T, Haukohl J, Marxen U. Municipal solid waste incineration: World Bank technical guidance report. Washington, DC: The World Bank; 1999.
[9] Xin C, Zhang T, Tsai S-B, Zhai Y-M, Wang J. An Empirical Study on Greenhouse Gas Emission Calculations Under Different Municipal Solid Waste Management Strategies. Appl Sci 2020;10(5):1673. https://doi.org/10.3390/app10051673.
[10] Sunil Kumar,Snehalata Ankaram. Chapter 12 - Waste-to-Energy Model/Tool Presentation. Current Developments in Biotechnology and Bioengineering. Waste Treatment Processes for Energy Generation 2019, pp. 239-258. Doi: 10.1016/B978-0-444-64083-3.00012-9.
[11] Lombardi L, Carnevale E, Corti A. A review of technologies and performances of thermal treatment systems for energy recovery from waste. Waste Manag 2015;37:26–44. https://doi.org/10.1016/j.wasman.2014.11.010.
[12] Zhang Ha, Siyuan Yu, Shao L, He P. Estimating source strengths of HCl and SO2 emissions in the flue gas from waste incineration. J Environ Sci 2019;75:370–7. https://doi.org/10.1016/j.jes.2018.05.019.
[13] Sorell G. The role of chlorine in high temperature corrosion in waste-to-energy plants. Mater High Temp 1997;14(3):207–20. https://doi.org/10.1080/09603409.1997.11689546.
[14] Bogale W, Viganò F. A Preliminary Comparative Performance Evaluation of Highly Efficient Waste-to-Energy Plants. Energy Procedia 2014;45:1315–24.
[15] Main, A, Maghon, T. "Concepts and Experiences for Higher Plant Efficiency With Modern Advanced Boiler and Incineration Technology." Proceedings of the 18th Annual North American Waste-to-Energy Conference. 18th Annual North American Waste-to-Energy Conference. Orlando, Florida, USA. May 11–13, 2010. pp. 33-40. ASME. 10.1115/NAWTEC18-3541.
[16] Ma W, Wenga T, Zhang N, et al. Full-scale experimental investigation of deposition and corrosion of pre-protector and 3rd superheater in a waste incineration plant. Sci Rep 2017;7:17549. https://doi.org/10.1038/s41598-017-17438-3.
[17] Liuzzo G, Verdone N, Bravi M. The benefits of flue gas recirculation in waste incineration. Waste Manag 2007;27(1):106–16.
[18] Eboh FC, Andersson B-Å, Richards T. Economic evaluation of improvements in a waste-to-energy combined heat and power plant. Waste Manag 2019;100:75–83.
[19] Poma C, Verda V, Consonni S. Design and performance evaluation of a waste-to-energy plant integrated with a combined cycle. Energy 2010;35(2):786–93.
[20] Bianchi M, Branchini L, De Pascale A, Falchetti M, Fiore P. Advanced Waste-to-energy Steam Cycles. Energy Procedia 2014;45:1205–14.
[21] Chen H, Zhang M, Xue K, Gang Xu, Yang Y, Wang Z, et al. 116893. ISSN 2020;0360–5442. https://doi.org/10.1016/j.energy.2019.116893.
[22] Carneiro MLN, Gomes MSP. Energy, exergy, environmental and economic analysis of hybrid waste-to-energy plants. Energ Conver Manage 2019;179:397–417.
[23] Bianchi M, Branchini L, Cesari S, De Pascale A, Melino F. Repowering existing under-utilized WTE power plant with gas turbines. Appl Energy 2015;160:902–11.
[24] Towler, G. and R. Sinnott, Chemical engineering design: principles, practice and economics of plant and process design. 2021: Butterworth-Heinemann.
[25] Bakar SH, Hamid MK, Alwi SR, Manan ZA. A simple case study on application in synthesising a feasible heat exchanger network. Chem Eng Trans 2017;56:157–62.
[26] Jack TA, Oko COC. Exergy and exergoeconomic analysis of a municipal waste-to-energy steam reheat power plant for Port Harcourt city. Int J Ambient Energy 2018;39(4):352–9. https://doi.org/10.1080/01430750.2017.1305447.
[27] Regulgadda P, Nater GF, Dincer I. Exergy Analysis of a Thermal Power Plant with Measured Boiler and Turbine Losses. Appl Therm Eng 2010;30:970–6. https://doi.org/10.1016/j.applthermaleng.2010.01.008.
[28] Rayaprolu, K., 2009, Boilers for power and process. 811 Pages 488 B/W Illustrations.
[29] Auracher, H., Thermal design and optimization: Adrian Bejan, George Tsatsaronis and Michael Moran John Wiley & Sons, Inc.(1996) 542 pp., $64.95, ISBN 0-471-58467-3. 1996, Elsevier.
[30] Babaei Jamnani M, Kardgar A. Energy-exergy performance assessment with optimization guidance for the components of the 396-MW combined-cycle power plant. Energy Sci Eng 2020;8(10):3561–74.
[31] Xiaoqu Han, Ming Liu, Kaili Wu, Weixiong Chen, Feng Xiao, Junjie Yan, Exergy analysis of the flue gas pre-dried lignite-fired power system based on the boiler with open pulverizing system, Energy, Volume 106.
[32] Li G, et al. Advanced exergy analysis of ash agglomerating fluidized bed gasification. Energ Conver Manage 2019;199:111952.
[33] Aljundi IH. Energy and exergy analysis of a steam power plant in Jordan. Appl Therm Eng 2009;29(2-3):324–8.
[34] Sadeghi M, Chitsaz A, Mahmoudi SMS, Rosen MA. Thermoeconomic optimization using an evolutionary algorithm of a trigeneration system driven by a solid oxide fuel cell. Energy, Elsevier 2015;89(C):191–204.
[35] Niessen, W.R., Combustion and incineration processes: applications in environmental engineering. 2010: CRC Press.